Available online at **www.ijmrhs.com**

ISSN No: 2319-5886

International Journal of Medical Research & Health Sciences, 2019, 8(2): 41-49

Laser Biosensor as for Pregnancy Test by Using Photonic Crystal Fiber

Belal Sara J[1]*, Alameri Layla M[2], Rashid Fareed F[1] and Mansour Tahreer S[2]

[1] *Institute of Laser for and Optoelectronic Engineering, University of Technology, Baghdad, Iraq*

[2] *Institute of Laser for Postgraduate Studies, University of Baghdad, Baghdad, Iraq*

**Corresponding e-mail: Sonako54@gmail.com*

ABSTRACT

The use of laser and optoelectronics concepts to develop biological detection systems is the goal of this work. A biosensor based on one of the interferometer techniques, Mach-Zhender interferometer (MZI) technique, and the using of the laser beam is developed for pregnancy detection or pregnancy hormone, Human chorionic gonadotropin (HCG), increasing. A part of photonic crystal fiber (PCF) with 3 different lengths (1.5 cm, 1.0 cm, and 0.5 cm) has been collapsed with 2 conventional single mode fibers (SMFs) to achieve MZI technique, Micro-holes collapsing and make high sensitive regions for the optical properties (refractive index and absorption) in the urine sample. This type of laser biosensor depends on light intensity measurement through a modified optical fiber. The sensing region is immersed in different urine samples of pregnant female and non-pregnant female. Biological changes in the urine sample due to the HCG increasing lead to a change in the optical properties (refractive index and absorption) of the urine sample. The results showed that the increasing of pregnancy hormones leads to an increase in the refractive index for a urine sample and a decrease in the intensity of the output laser beam. From this test, the calibration curve of laser biosensor for a pregnancy test or pregnancy detection has been found. The sensitivities of the laser biosensor with a refractive index in the range (1.33864-1.34257) at (1.5 cm, 1.0 cm, and 0.5 cm) PCF length are 61.142 ABS/ RIU, 4.5132 ABS/RIU and 2.888 ABS/RIU, respectively. Thus, the highest sensitivity was found for the (1.5 cm) photonic crystal fiber length.

Keywords: Laser biosensor, Pregnancy test, PCF, detection, HCG, MZI

INTRODUCTION

The laser has a big importance in biological application [1]. Since the invention of the laser, many efforts have been made to apply this instrument in medicine and biology. Although lasers have traditionally been used in medicine as therapeutic devices, there has been a recent interest in using them as diagnostic tools. Most existing laser-based detection methods used in large-scale instruments can be miniaturized by using optical fibers. The laser detection technique based on evanescent waves is widely used in biosensors [2]. In the last few years, laser biosensors have become very important tools in many areas like analytical biochemistry, pharmaceutical study and development, food/ environmental observing and diagnostic testing [3,4]. Designing laser biosensor components are less expensive, more precise, and more accurate than test strips. There is a series of biosensors which use laser-based detection methods like Surface Plasmon Resonance (SPR), Fiber optics, waveguides, and so on. Laser-based biosensors have an important role in many fields, including immunoassays and drug screening due to their high sensitivity and precision [5].

This study aims to design and construct a laser biosensor based Mach-Zehnder interferometer technique (Micro-Holes Collapsing) using a solid core-photonic crystal fiber (LMA-10) with different PCF lengths and use it for pregnancy detection in the urine sample.

PATIENTS AND METHODS

Laser Biosensor based on Mico-Hole Collapsing Technique

Micro-hole collapsing is a simple kind of Mach-Zehnder interferometer (MZI) because its fabrication only needs cleaving and splicing the optical fiber [6]. By changing the parameters of the fusion splicing, the collapsed region can

be controlled [7]. At the region where the holes are collapsed, there is no fiber cladding and the photonic crystal fiber is no more in single mode. This way can be designed by splicing PCF between two SMF [8].

At the first collapsed region, the air hole is completely collapsed; the beam mode of the core is diffracted and worked as a splitter. In the PCF core, the beam will be expanded and a part of core mode can be coupled to the PCF cladding modes at the collapsing region [9]. After propagating the length of the PCF (L) and when they reach of the second collapsed region, they will recombine [10].

By using Gaussian beam approximation, broadening of a fundamental mode can be measured [11]. Mode field diameter (MFD) at the splicing point (z) can be calculated from:

$$MFD = 2w\sqrt{1+\left(\frac{z\lambda}{\pi n w^2}\right)} \quad (1)$$

Where n is the refractive index of the core (pure silica), λ is the light wavelength and w is the light spot size.

In general, interference pattern which is depending on the length of optical path shows the displacement between two-arms of interferometer because core mode has a higher effective index than the cladding mode [12]. Therefore, the physical lengths of interferometer arms are similar; the phase different is directly related to the difference between the effective indices of the cladding and core mode [13].

The intensities of core and the cladding modes can be measured as function of a physical length (L), wavelength and phase difference (φ):

$$I = I_{CO} + I_{CL} + 2\sqrt{I_{CO}I_{CL}}\cos\Delta\varphi \quad (2)$$

Where, I_{CO}, I_{CL} is the mode intensities of cladding and core mode [14]. The phase difference between the sensing cladding and core modes is described by:

$$\Delta\varphi = 2\pi / \lambda\ \Delta n.L \quad (3)$$

Where L is the interaction length (the sensing area length), is the wavelength in the vacuum, and $\Delta n = n_{eff\ core} - n_{eff\ clad}$ is the change in the effective refractive index of the mode.

By changing the length of the photonic crystal fiber, the fringe or period spacing in these interferometers can be easily controlled [15].

Experimental Works

Absorption measurement for urine sample: UV-visible-NIR spectrophotometer (SP-8001) which runs in a wavelength range from 190 nm to 1100 nm has been applied to measure the Ultraviolet-Visible absorption spectra of the biological samples shown in Figure 1. The sample of urine has been put in the quartz cuvette to obtain the absorption spectrum. The laser source is selected according to the obtained absorption spectrum.

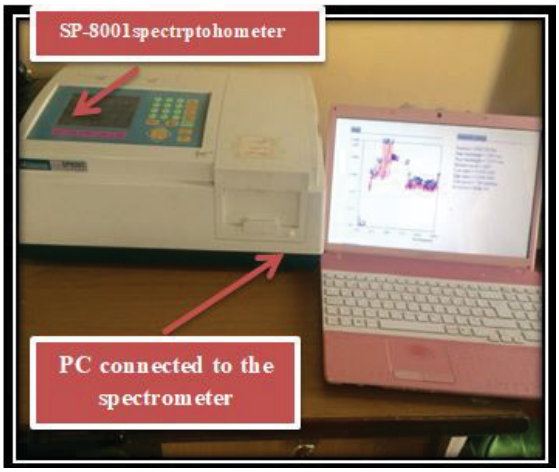

Figure 1 Experimental setup for light absorption measurement

Refractive Index Measurement for Biological Samples

The refractive index of the urine samples was measured by Abbe refractometer. A few drops of the liquid to be examined are placed on the polished surface of the lower refracting prism and upper incident prism is closed, so the liquid is distributed on the surface of refracting prism.

The experimental reading can be corrected for temperature using the following equation:

$n_{D20} = n_{DT} + 0.00045\ (T\text{-}20°C)$

Where (n_{DT}) is the experimental refractive index value measured at temperature T and (n_{D20}) is the refractive index value measured at 20°C.

Selectivity of the Urine Samples by using the General Urine Examination (GUE)

Taking different urine samples from different females (non-pregnant and pregnant) to examine them the urine compositions with a microscope shown in Figure 2.

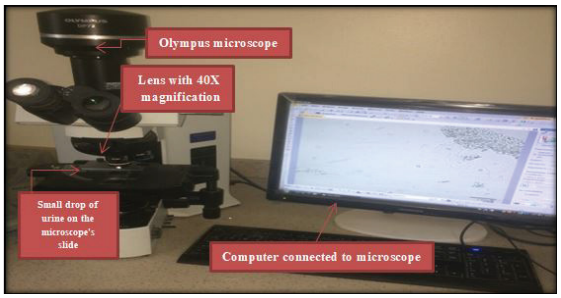

Figure 2 Experimental setup for microscope urine examination

A small drop of urine has been examined by scanning the average number of red blood cell in the high power field (RBC/hpf), white blood cell in the high power field (WBC/hpf), casts/hpf, bacteria, yeasts, crystals, epithelial cells, etc.

This exam helps us to select urine samples from different pregnant and non-pregnant females which have the same healthy ranges for urine compositions rate.

Design a Laser Biosensor For pregnancy Test based on Transmission

The transmission part which consists of a short part of a PCF, which is shown in Figure 3, spliced with SMF-28 in both ends is involved in the Mach-Zehnder modal interferometer. A Fujikura (FSM-60S) splicing machine was used to fusion splice PCF (LMA-10) and SMF-28.

The standard single mode fiber (SMF-28) has been used and the photonic crystal fiber (LMA-10) which has a solid core surrounding by 4 circles of air holes ordered in a hexagonal pattern. It has (125 ± 2) μm outer cladding diameter, (10.1 ± 0.5) μm core diameter, 3.1 μm air hole diameter and 6.6 μm hole to hole spacing.

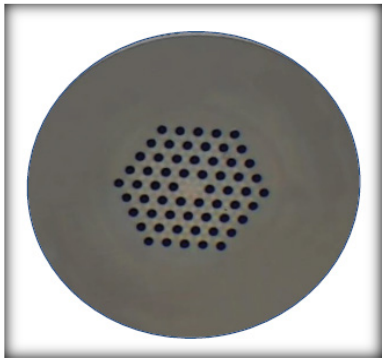

Figure 3 The cross-section of top view for the PCF (LMA-10)

Generally, photonic crystal fiber was spliced with SMF-28 on both sides by using a fusion splicing machine. The fusion time and fusion power have been changed. Based on trial and error, the collapsed region in this work was (250-300) µm.

In the first spliced zone, the air holes are totally collapsed. The input core mode passes through the first collapsed zone, and the diameter of its mode field is expanded and causes excitation of the cladding and core modes. Then, the cladding and core modes couple at the second spliced zone, after passing within the distance L (the length of the PCF).

The laser source has a wavelength of (650 nm) with an output power of (2.4 mW) and stable power supply. This laser has been used due to the absorption spectrum of normal urine sample which covers the wavelength region centered at 650 nm as will been shown later.

The urine sample has been put above the PCF sensor. Three PCFs were used with different lengths (1.5 cm, 1.0 cm, 0.5 cm). The transmission spectrum of the sensor was monitored using an optical spectrum analyzer (ocean optics HR2000).

In this work, various urine samples lead to change the effective index of the modes of fiber cladding. This change of the refractive index of the cladding (ncl) occurs with respect to the value of the refractive index of urine samples which change transmission intensity. Figure 4 shows a photographic picture for the experimental set-up.

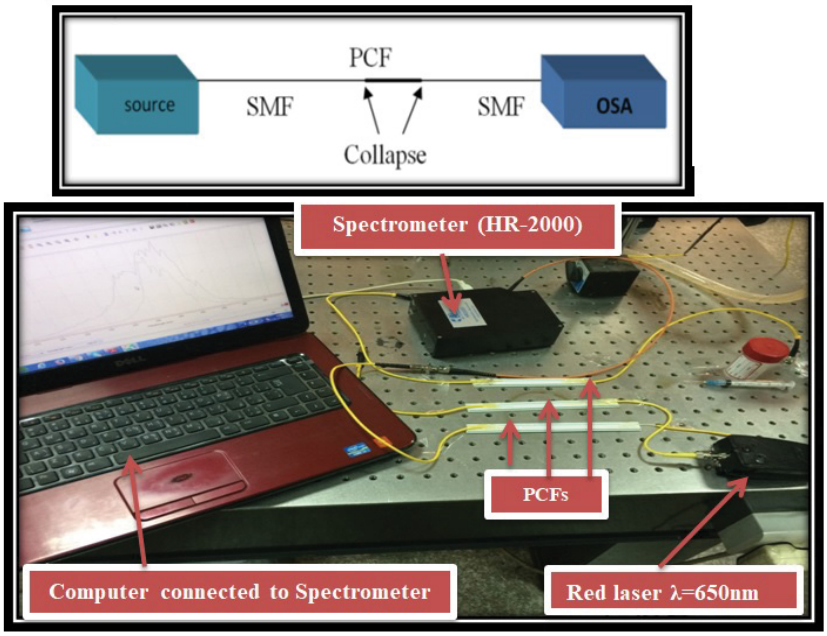

Figure 4 (a) The schematic of the proposed sensors (b) the experimental set-up of the transmission model for urine samples

RESULTS AND DISCUSSION

Absorption Spectra for the Urine sample

The absorption spectra for urine sample are measured using (T60 UV-VIS) spectrophotometer to select the suitable wavelength of a laser source for the detection set-up. Figure 5 shows the absorption spectra for a urine sample.

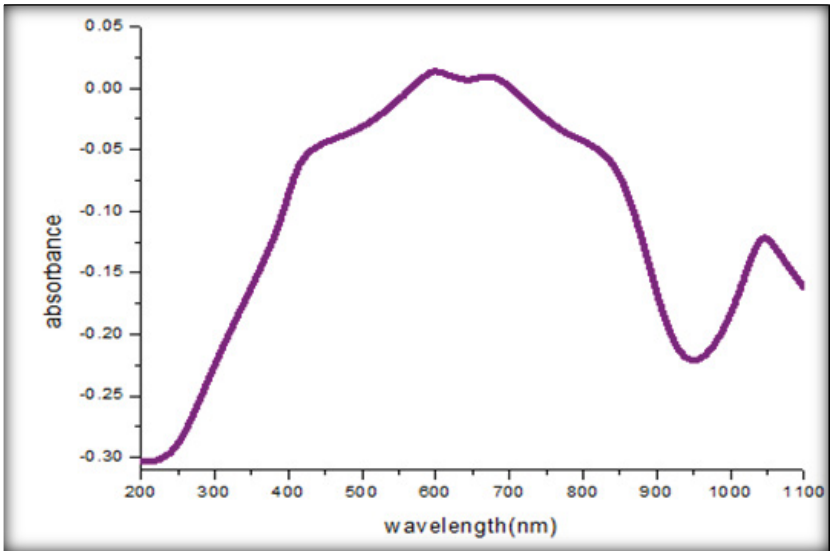

Figure 5 Absorption spectrum for a normal urine sample

From Figure 5 the maximum absorbance of the urine sample noticed in the wavelengths ranges 590 nm to 670 nm. Thus, a red diode laser with 650 nm wavelength was used as a laser source for laser biosensor of urine test applications.

Refractive Index of the Selective Urine Samples

The results of general urine examination (GUE) and refractive index measurement for non-pregnant and pregnant female urine samples are shown in Table 1.

Table 1 The results of general urine examination (GUE) and refractive index measurement for non-pregnant and pregnant female urine samples

Statue Of The Female	Results of (GUE)								Refractive Index
	Glucose	Protein	PH	Pus Cells	RBCs	Crystals	Epithelial Cells	Uric Acid	
Non-Pregnant no.1	Normal	Normal	Acidic	0-1	0-1	0-1	0-1	0-1	1.33864
Non-Pregnant no.2	Normal	Normal	Acidic	0-1	0-1	0-1	0-1	0-1	1.34008
Pregnant no.1	Normal	Normal	Acidic	0-1	0-1	0-1	0-1	0-1	1.34235
Pregnant no2	Normal	Normal	Acidic	0-1	0-1	0-1	0-1	0-1	1.34257

According to Table 1, it can be noticed that although the selected urine samples have the same compositions rate but the refractive indices of the urine samples are proportionally increased in the cases of the pregnancy. This change is due to the pregnancy hormone, HCG, which increases in the pregnant urine sample.

Pregnancy Test using Laser Biosensor

The proposed sensors with 1.5 cm, 1.0 cm, and 0.5 cm PCF length been used for comparison between the output spectrum of the laser (λ=650 nm) after passing through non-pregnant and pregnant urine samples. The results are monitored by an optical spectrum analyzer (ocean optics HR2000) connected to a computer as shown in Figure 6.

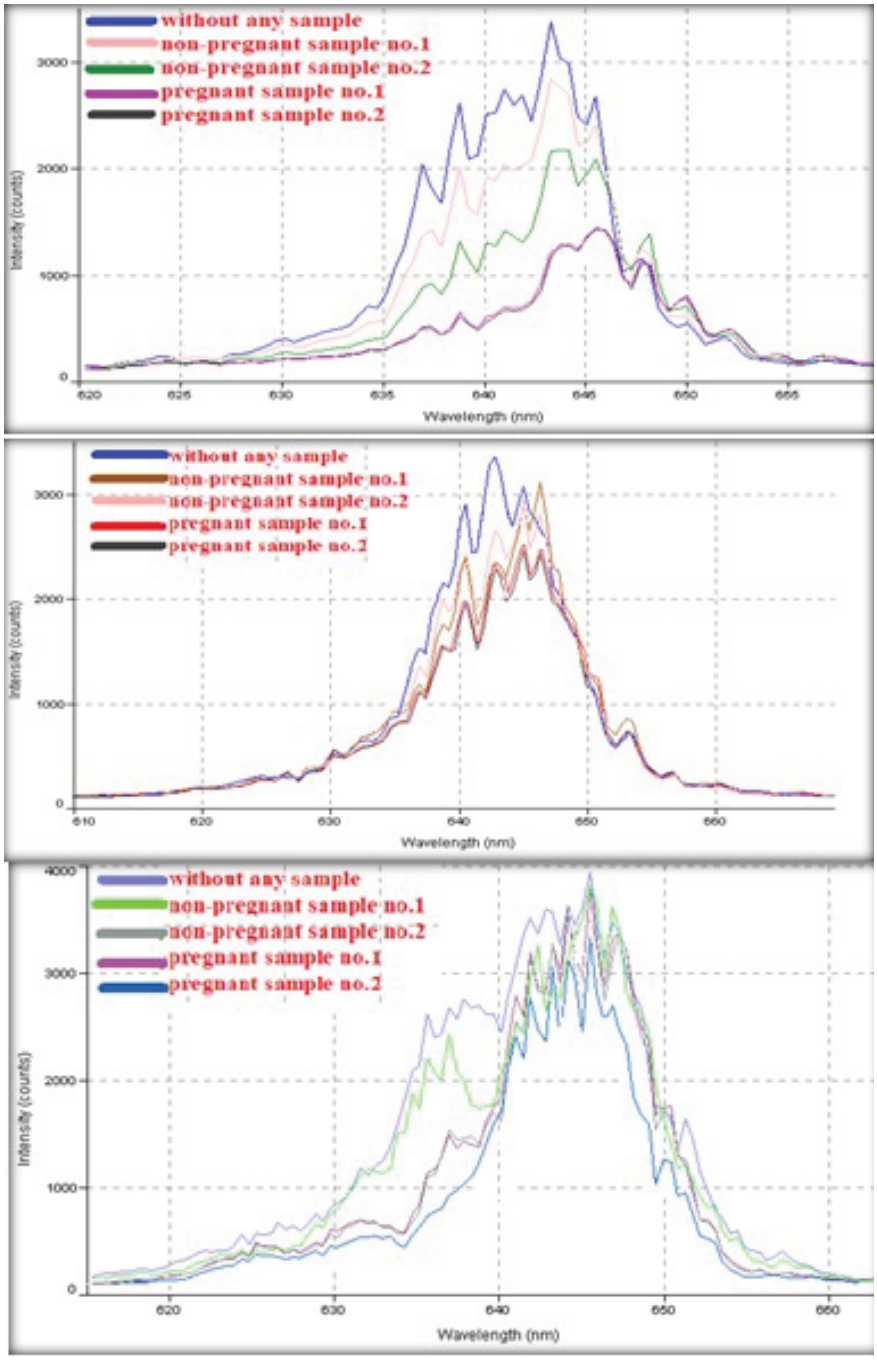

Figure 6 The transmission spectra at different urine samples of different non-pregnant and pregnant females at (A) 1.5 cm (B) 1 cm (C) 0.5 cm PCF length

From the previous figure, sharp fringes appear with an increase in the phase difference as shown in equation 2; the maximum transmission intensities, so the absorbance, after the laser passed through the urine samples are changed due to the increase in the refractive indices hence the HCG increases subsequently.

Relationship between the Sensitivity of Biosensor and the PCF Length

The sensitivity of the proposed sensors is measured from the slope of the graph between the refractive indices and absorption of the urine samples for the laser diode which are found by using these sensors. Relationships between the refractive index of the urine samples and absorbance are shown in Figure 7 below:

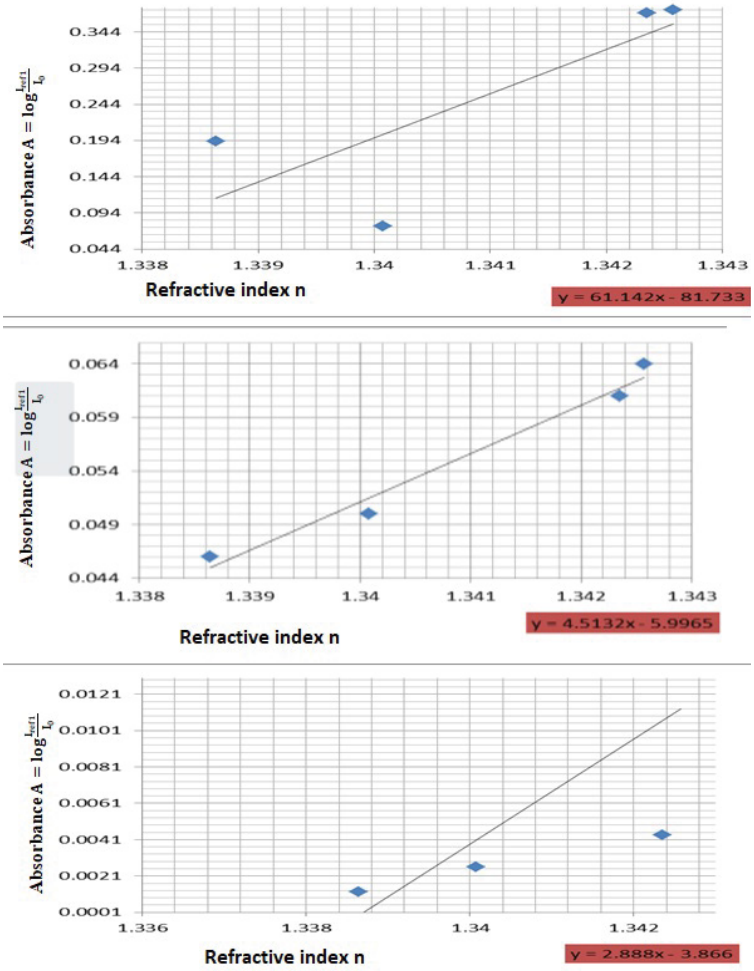

Figure 7 Calibration curve of laser biosensor as pregnancy tester at (a) 1.5 cm (b) 1 cm (c) 0.5 cm LMA-10 PCF length

The sensitivities of the proposed laser biosensors are calculated by the Excel program. The relationship between the sensitivity and PCF length is shown in Figure 8 below.

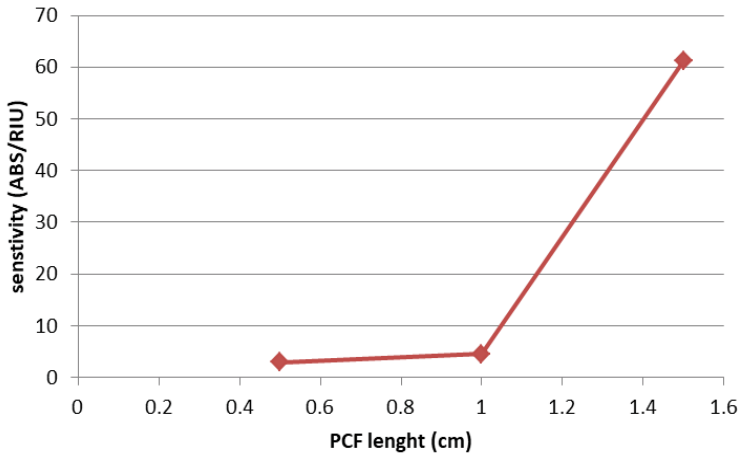

Figure 8 Relation between sensitivity and length of LMA-10 photonic crystal fiber

As a result, the maximum sensitivity at 1.5 cm PCF length is equal to 153ABS/RIU. This is because of the increase

in the interaction length as the length of the PCF goes from 0.5 cm to 1.5 cm. As a result, sharp fringes shall appear with an increase in the phase difference as shown in equation 2.

CONCLUSION

In conclusion, the followings points have been observed:

- The absorption spectrum of the urine sample showed that maximum absorbance of the blood sample is for wavelengths in the range (590-670) nm
- The presence of the pregnancy causes an increase in the refractive index of the urine sample, thus the intensity of the output beam is lower than the intensity for a non-pregnant urine sample. This is because of the presence of pregnancy HCG hormone
- The sensitivities of the laser biosensor refractive index in the range (1.33864-1.34257) at (1.5 cm, 1.0 cm, and 0.5 cm) PCF length are 61.142 ABS/RIU, 4.5132 ABS/RIU and 2.888 ABS/RIU, respectively
- The sensitivity (or variation of the intensity) is increased by increasing the length of the PCF within the range of the fiber used

DECLARATIONS

Conflict of Interest

The authors declared no potential conflicts of interest with respect to the research, authorship, and/or publication of this article.

REFERENCES

[1] Banerjee, Argha, et al. “Fiber optic sensing of liquid refractive index.” *Sensors and Actuators B: Chemical,* Vol. 123, No. 1, 2007, pp. 594-605.

[2] Jollivet, Clémence, et al. “Comparative study of light propagation and single-mode operation in large-mode area fibers designed for 2-μm laser applications.” *Optical Engineering,* Vol. 54, No. 1, 2014, p. 11006.

[3] Chistiakova, Maria V., Ce Shi, and Andrea M. Armani. “Label-free, single molecule resonant cavity detection: A double-blind experimental study.” *Sensors,* Vol. 15, No. 3, 2015, pp. 6324-41.

[4] Qiu, Xianbo, et al. “A low-cost and fast real-time PCR system based on capillary convection.” *Slas Technology: Translating Life Sciences Innovation,* Vol. 22, No. 1, 2017, pp. 13-17.

[5] Shaker, Maan M., Mahmood Sh Majeed, and Raid W. Daoud. “A new approach for representing photonic crystal fiber index profile to determine their optical characteristics.” *Energy, Power and Control (EPC-IQ), 2010 1st International Conference on*. IEEE, Vol. 7, No. 1, 2010, pp. 268-72.

[6] Nazeri, K, et al. “Photonic crystal fiber based refractive index sensors.” A*dvanced Materials-TechConnect Briefs,* Vol. 3, 2017, pp. 203-06.

[7] Rifat, Ahmmed A., et al. “Highly sensitive multi-core flat fiber surface plasmon resonance refractive index sensor,” *Optics Express*, Vol. 24, No. 3, 2016, p. 2485.

[8] Sadana, N, et al. “Detection of cancer biomarkers by biosensors: Part II.” *Biomarkers and Biosensors*, 2015, pp. 109-67.

[9] Valadez, Angela M., et al. “Evanescent wave fiber optic biosensor for Salmonella detection in food,” *Sensors*, Vol. 9, No. 7, 2009, pp. 5810-24.

[10] Slussarenko, Sergei, et al. “Guiding light via geometric phases,” *Nature Photonics*, Vol. 10, No. 9, 2016, pp. 571-75.

[11] Han, Tingting, et al. “Avoided-crossing-based ultrasensitive photonic crystal fiber refractive index sensor.,” *Optics letters*, Vol. 35, No. 3, 2010, pp. 2061-63.

[12] Xu, F, et al. *Sensors based on microstructured optical fibers modal interferometers,* 2017.

[13] Amma, Yoshimichi, et al. "Fusion splice techniques for multicore fibers," *Optical Fiber Technology*, Vol. 35, 2017, pp. 72-79.

[14] Song, Qinghai, et al. "Detection of nanoscale structural changes in bone using random lasers." *Biomedical Optics Express*, Vol. 1, No. 5, 2010, pp. 1401-07.

[15] Renversez, Gilles. "Foundations of photonics crystal fibres: A review." *Advanced Photonics*, 2014.